https://doi.org/10.1016/j.msea.2013.08.043

Multi-layer laminated Pd-based metallic glass with enhanced plasticity

J. Ma [1,2], K.C. Chan [1,*], L. Xia[1], S.H. Chen[1], F.F. Wu[1], W.H. Li [3] and W.H. Wang [2]

[1] Advanced Manufacturing Technology Research Centre, Department of Industrial and Systems Engineering, The Hong Kong Polytechnic University, Hung Hom, Hong Kong

[2] Institute of Physics, Chinese Academy of Sciences, Beijing 100190, People's Republic of China

[3] School of Materials Science and Engineering, Anhui University of Technology, Ma'anshan 243002, People's Republic of China

* Corresponding author. Tel.: +852 27664981. E-mail address: kc.chan@polyu.edu.hk (K.C. Chan).

Abstract

We have demonstrated, for the first time, the enhanced plasticity of multi-layer Pd-based bulk metallic glasses (BMGs) synthesized by thermoplastic bonding (TB). The structural relaxation was minimized by using a low bonding temperature and a very short holding time. As compared to the as-cast and the two-layer BMG samples, the three-layer samples achieve larger plasticity. The fracture morphology of the multi-layer samples exhibit radiating-ridge patterns as compared to the river-like cell patterns observed in as-cast BMGs. The enhanced plasticity is due to the blocking effect of the bonding interface for the propagation of shear bands. Our research opens a promising way to synthesize BMGs with larger size and enhanced plasticity for potential structural applications.

Keywords: Metallic glass; Thermoplastic bonding; Plasticity; Blocking effect; Structure relaxation.

1. Introduction

Since the discovery of bulk metallic glasses (BMGs) in the 1960s [1], these materials have attracted tremendous research interest due to their unique properties, such as high specific strength, good corrosion resistance, soft magnetic properties and unique net-shape formability [2-6]. However, the limited sample size and room-temperature brittleness are still two of the major issues hindering their applications [7,8]. In the past decades, although there have been extensive research efforts to study the deformation mechanisms of BMGs, the intrinsic brittleness of monolithic BMGs still remains unresolved. [9-11]. On the other hand, in order to address the issue of limited sample size, much research effort has been spent in developing joining technologies, such as friction welding [12-15], spark welding [16] and electron beam welding [17,18]. These methods have been shown to be able to bond BMGs, but they are far from satisfactory because of defects that may arise from the processes, such as poor surface finish and crystallization [19,20]. There is a need to further improve the bonding technology for BMGs.

BMGs are known to behave like the Newtonian viscous flow and show superplasticity when the temperature is increased to the supercooled liquid region (SLR) [21]**,** which is a temperature window between the glass transition temperature T_g and the crystallization temperature T_x [21]. This nature allows BMGs to be thermoplastic formed,

and has been proven to be an unique material processing method having many advantages, including cost reduction and weight saving, compared with conventional methods [5,22]. Based on these characteristics, a number of researchers have demonstrated that BMGs can be joined by thermoplastic bonding [12-20]. However, this process will induce a certain degree of structural relaxation, leading to a deterioration of the plasticity. In order to apply this bonding technique for synthesizing larger BMGs, it is essential and challenging to improve the plasticity of bonded BMGs.

In present work, we demonstrate, for the first time, the enhancement of the plasticity of multi-layer BMGs synthesized by thermoplastic bonding. The PdNiCuP bulk glassy alloy was chosen for present study, due to the fact that this BMG has been shown to have excellent thermoplastic forming ability, large SLR and good resistance to oxidation and crystallization [21,23].

2. Experimental procedure

PdNiCuP BMG sheet with a thickness of 1 mm was prepared from a master alloy with nominal composition Pd 40 at.%, Ni 10 at.%, Cu 30 at.%, and P 20 at.% by a conventional water cooled copper mould casting process. The as-cast glassy sample was cut and sawn into a required dimension (15 mm × 4 mm ×1 mm) for bonding. The BMG specimens were first polished by hand with abrasive paper up to 1200 grit and then by a polishing machine with 1.5 μm diamond paste.

The schematic setup of TB, performed on Gleeble 3500 thermal-mechanical testing system, is shown in Fig. 1. Multi-layer BMG sheets were stacked together and then

heated to the bonding temperature at a heating rate of 60 K/min by applying electric current to the samples under a vacuum environment. Thermocouples at the two ends are used to avoid overheating or underheating of the samples. Afterwards, a force is applied and held for a period of time for bonding. The parameters controlling the process are bonding temperature, holding time and initial pressure. Since the TB process has to be conducted at elevated temperatures, it is important to avoid any crystallization and to minimize structural relaxation during the process. The temperature and time dependent transformation from an amorphous to a crystalline state of this BMG speciman can be summarized in a temperature-time-transformation (TTT) diagram which was determined by isothermal crystallization studies [24]. From the TTT diagram, it can be easily estimated how much time is taken to crystallize a $Pd_{40}Cu_{30}P_{20}Ni_{10}$ BMG at certain temperature. In our work, two processing temperatures, T_1=583 K and T_2=593 K, which are very close to T_g are selected in order to minimize structural relaxation and crystallization. They are 10 K and 20 K higher than T_g respectively. Their corresponding crystallization times t_{T_1} and t_{T_2} are no less than 7000 s and 4500 s, as estimated from the TTT diagram [25]. In the present work, since the Pd-based MG has excellent flow ability in its SLR, it allows very little holding time. The selected holding times from 10 s to 10 min are much shorter than the crystallization time and the holding time used by other researchers for TB [26-29]. It can effectively minimize the structural relaxation during the process. The initial pressure is another parameter affecting the structural relaxation. As compared to the pressure used by other researchers, very low initial pressures (50 and 100 MPa) were used in this study [26-29]. The values of these three

parameters used in the present experiments are summarized Table I. The inset of Fig. 1 shows the multi-layer BMG sheet before TB (left) and BMG plate after TB (right).

The amorphous nature of the as cast and TB treated Pd-based BMG samples was ascertained by x-ray diffraction (XRD; Rigaku SmartLab) with Cu K_α radiation and differential scanning calorimetry (DSC; Perkin–Elmer DSC-7) at a heating rate of 20 K/min. This showed a glass transition temperature (T_g) of 573 K and a crystallization temperature (T_x) of 653 K. The mechanical performance of the as cast and TB treated BMG samples was measured on an electromechanical MTS 810 equipment. The bonding quality between the multi-layer BMG sheets after TB, and the fracture morphologies of them were investigated by scanning electron microscope (SEM) observation, performed on Jeol 6490 SEM instrument.

3. Results and discussions

The inset of Fig. 1 shows the photograph of BMG product by TB, in which it can be seen to have a regular shape, and unlike in the welding process [12-18], almost no post processing such as polishing or wire electrical discharge machining (WEDM), is needed. The XRD patterns and DSC curves of the as-cast and the bonded BMG samples, which are labeled from 0# to 6#, are presented in Fig. 2a and b. It is clearly seen that they keep fully amorphous structures after TB, even the three-layer samples 5# and 6#. To examine the bonding quality of the multi-layer BMG sheets, the interfaces between the layers of the bonded BMGs are observed by SEM. As shown in Fig. 2c, the polished cross section of each bonded sample, from 1# to 6#, is highlighted by the dashed line. No interface is

observed in these SEM images, showing the achievement of good bonding between the BMG sheets. It should be noticed that samples 5# and 6# consist of three layers and sound bonding is also obtained. There have been great efforts spent by other researchers to achieve a good bonding quality. For the bonding of $Zr_{52.5}Cu_{17.9}Ni_{14.6}Al_{10}Ti_5$ in its SLR, a pressure of 11.55 MPa was used, but the holding time was 60 min at 27 K above its T_g temperature [26], while Yamaura et al. used a pressure up to 211 MPa for 5 min at the temperature of 37 K above T_g in the bonding of $Zr_{55}Al_{10}Ni_5Cu_{30}$ metallic glass ribbon and an SUS316L porous substrate [28]. However, in present study, the Pd-based BMG could be firmly bonded under a low pressure of 50 MPa and at a temperature of only 10 K above T_g with a very short holding time of 10 s. This indicates the excellent TB ability of the Pd-based BMG. The low operating temperature and short holding time in the TB of Pd-based BMGs have great significance to their plasticity after TB, because it will minimize the structure relaxation.

The mechanical performance of the BMG samples after TB is also investigated. Figure 3 presents the Vickers hardness of the as-cast and bonded samples which is measured at different positions of the cross section with a load of 500 g and a loading time of 10 s. It can be seen from Fig. 3a that the hardness of the bonded samples (designated by solid circles) is a little higher than the as-cast one (designated by solid squares). The average Vickers hardness (see the dashed line in Fig. 3a) of the bonded samples from 1# to 6# is 534.0 Hv, about 4.5% higher than the as-cast one 0# which is 510.75 Hv. The hardness distribution across the bonding interface is also examined by taking 6# as an example, which is shown in Fig. 3b. The inset demonstrates the positions

measured on the cross section. We can see that the hardness is distributed uniformly (even better than the as-cast one 0#) across the bonding interface and there is no sudden change, indicating that the TB process has strongly joined the multi-layer BMG sheets together [26].

Figure 4a presents the stress and strain curves of the as-cast and bonded BMG samples of the dimension of 1 mm × 1 mm ×2 mm under compression testing (strain rate = 2×10^{-4} s^{-1}). It can be seen that the fracture behaviour of the as-cast speciman is a typically brittle one, with almost no plasticity observed, and a fracture strength of 1326 MPa. In contrast, the BMG samples after TB reveal different behaviour. While the two-layer (e.g. 3#) BMG has a slight improvement in the plasticity, the three-layer BMG samples can achieve more obvious improvement. When comparing the plasticity of sample 5# to sample 6#, the latter has achieved a very significant improvement. Apparently, the difference in holding time during TB (see Table I) for 5# and 6# is the main reason for their different mechanical responses. The holding time for 5# is much longer than 6#, which results in more structure relaxation and induces the annihilation of the free volumes in the glass, leading to its brittleness. It becomes essential to carefully control the holding time so as to avoid excessive structure relaxation. To understand more clearly the difference in plasticity, the fracture morphologies of different BMG samples are characterized (see Fig. 4b). The full views of the fracture sections of samples 0#, 3# and 6# are shown in the top row of Fig. 4b, and the corresponding close-up views (highlighted by the dashed squares) are presented in the bottom row, respectively. We can clearly see that the fracture morphology of the as-cast BMG reveals river-like cell

patterns (see the left of Fig. 4b) which is typical and usually found in brittle BMGs. However, the fracture morphology of the multi-layer samples exhibits radiating-ridge patterns (see the middle and right of Fig. 4b). The schematic diagram for the evolution from river-like cell patterns to radiating-redige patterns is illustrated in the inset of Fig. 4a. During the process of fracture, the existence of bonding interfaces in the BMG samples after TB may block the prolongation of the river-like cell pattern, resulting in the radiating-ridge pattern. The blocking effect of the interface is highlighted by the dashed ellipse in this inset. Furthermore, by comparing 3# with 6#, it is easy to find that the blocking effect is stronger when more interfaces are introduced, therefore, a larger density of radiating-ridge patterns could be created, which has good consistency with the SEM observations. In addition, the three-layer sample (6#), which shows plasticity also has larger dimple size compared with the others, indicating better mechanical performance [30]. The micro-scale hard regions in the metallic glasses, which can effectively block the propagation of shear bands and improve the plasticity, have also been found in inhomogeneous metallic glasses [31]. Based on the above discussions, the bonding interface (invisible in the SEM observations yet still existent) of the multi-layer BMGs after TB plays the important role of a blocker in the prolongation of the cell patterns and hence the mechanical properties are improved.

4. Conclusions

In this study, we have demonstrated that multi-layer Pd-based BMG can be prepared by the TB process. Owing to the good TB ability of this BMG, a lower temperature and

pressure and a much shorter time are needed for the preparation of multi-layer Pd-based BMGs. It does not only achieve excellent bonding quality, but also can minimize the structure relaxation during the process. As compared to the as-cast BMG, the multi-layer Pd-based BMG exhibits enhanced plasticity. The three-layer BMG samples have further demonstrated larger plasticity than the two-layer samples. By examining the fracture morphologies of different BMG samples, the enhancement is shown to be due to the blocking effect of the bonding interface for the propagation of shear bands.

Acknowledgements

The work described in this paper was supported by a grant from the Research Grants Council of the Hong Kong Special Administrative Region, China (Project No.: PolyU 511510). We thank Y. L. Pan, J. G. Wang and M. Gao for discussions and helping for experiments. J. Ma and W. H. Wang also thank the support of MOST 973 of China (Nr. 2010CB731603) and the NSF of China (51271195).

References

[1] W. Klement, R.H. Willens, P. Duwez, Nature 187 (1960) 869-870.

[2] A. Inoue, Acta Mater. 48 (2000) 279-306.

[3] W.L. Johnson, MRS Bull. 24 (1999) 42-56.

[4] A. Inoue, A. Takeuchi, Mater. Trans. JIM 43 (2002) 1892-1906.

[5] J. Schroers, Adv. Mater. 22 (2009) 1566-1597.

[6] W.H.Wang, Prog. Mater. Sci. 57 (2012) 487-656.

[7] C.A. Schuh, T.C. Hufnagel, U. Ramamurty, Acta Mater. 12 (2007) 4067-4109.

[8] J. Xu, U. Ramamurty, E. Ma, JOM 62 (2010) 10-18.

[9] J. Eckert, J. Das, K.B. Kim, F. Baier, M.B. Tang, W.H. Wang, Z.F. Zhang, Intermetallics 14 (2006) 876-881.

[10] L.Y. Chen, Z.D. Fu, W. Zeng, G.Q. Zhang, Y.W. Zeng, G.L. Xu, S.L. Zhang, J.Z. Jiang, J. Alloys Compd. 443 (2007) 105-108.

[11] D.H. Bae, S.W. Lee, J.W. Kwon, X.D. Wang, S. Yi, Mater. Sci. Eng. A 449 (2007) 111-113.

[12] C.H. Wong, C.H. Shek, Scr. Mater. 49 (2003) 393-397.

[13] Y. Kawamura, Y. Ohno, Scr. Mater. 45 (2001) 279-285.

[14] T. Shoji, Y. Kawamura, Y. Ohno, Mater. Sci. Eng. A 375 (2004) 394-398.

[15] H.S. Shin, Y.J. Jeong, H.Y. Choi, H. Kato, A. Inoue, J. Alloys Compd. 434 (2007) 102-105.

[16] Y. Kawamura, Y. Ohno, Scr. Mater. 45 (2001) 127-132.

[17] Y. Kawamura, T. Shoji, Y. Ohno, J. Non-Cryst. Solids 317 (2003) 152-157.

[18] S. Kagao, Y. Kawamura, Y. Ohno, Mater. Sci. Eng. A 375 (2004) 312-316.

[19] Y. Kawahito T. Terajima, H. Kimura, T. Kuroda, K. Nakata, S. Katayama, A. Inoue, Mater. Sci. Eng. B 148 (2008) 105-109.

[20] J.J. Lewandowski, W.H. Wang, A.L. Greer, Philos. Mag. Lett. 85 (2005) 77-87.

[21] R. Busch, J. Schroers, W.H. Wang, MRS Bull. 32 (2007) 620-623.

[22] X.F. Wang, Z.C. Luo, X.B. Liu, J.G. Lin, Sci. Tech. Weld. Join. 13 (2008) 452-455.

[23] J. Yi, X.X. Xia, D.Q. Zhao, M.X. Pan, H.Y. Bai, W.H. Wang, Adv. Eng. Mater. 12

(2010) 1117-1122.

[24] J.F. Loffler, J. Schroers, W.L. Johnson, Appl. Phys. Lett. 77 (2000) 681-683.

[25] J. Ma, X. Zhang, W.H. Wang, J. Appl. Phys. 112 (2012) 024506.

[26] P.H. Kuo, S.H. Wang, P.K. Liaw, G.J. Fanc, H.T. Tsang, D.C. Qiao, F. Jiang, Mater. Chem. Phys. 120 (2010) 532-536.

[27] M. Ohta, A.E. Berlev, V.A. Khonik, Phil. Mag. 83 (2003) 3463-3471.

[28] S. Yamaura, H. Kimura, A. Inoue, Mater. Trans. 48 (2007) 273-276.

[29] H. Somekawa, A. Inoue, K. Higashi, Scr. Mater. 50 (2004) 1395-1399.

[30] X.K. Xi, D.Q. Zhao, M.X. Pan, W.H. Wang, Y. Wu, J.J. Lewandowski, Phys. Rev. Lett. 94 (2005) 125510.

[31] Y.H. Liu, G. Wang, R.J. Wang, D.Q. Zhao, M.X. Pan, W.H. Wang, Science 315 (2007) 1385-1388.

Figure captions

Fig. 1. Schematic drawing of the TB process for BMG. The inset shows the multi-layer BMG sheets before TB (left) and BMG plate after TB (right).

Fig. 2. (a) the XRD patterns and (b) the DSC curves of the as cast and TB treated BMG samples. (c) the SEM images of the section across the interface of multi-layer BMG samples after TB.

Fig. 3. (a) Vickers hardness on the section across the interface of BMG samples after TB compared with the as cast one. (b) Hardness distribution of 6# across the bonding interface compared with the as cast one.

Fig. 4. (a) Compression stress and strain curves of the as cast, two-layer (3#) and three-layer (6#) BMGs. The inset shows the blocking effect of the interface, causing the evolution of the fracture morphologies from river-like cell patterns to radiating-redige patterns. (b) The fracture morphologies of the as cast (0#), two-layer (3#) and three-layer (6#) BMGs. The top row are the full views and the bottom row are the corresponding close-up views (highlighted by dashed squares in the full views).

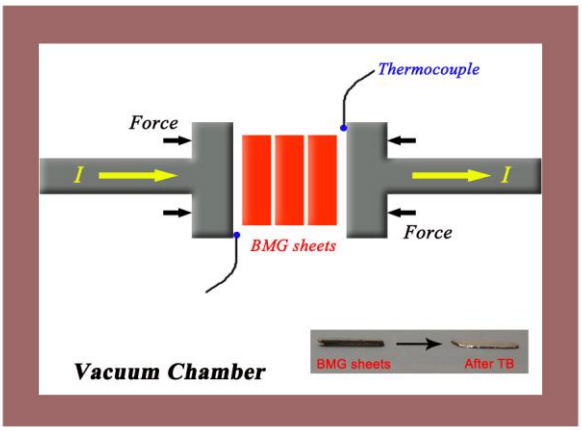

Figure 1. J. Ma *et al*

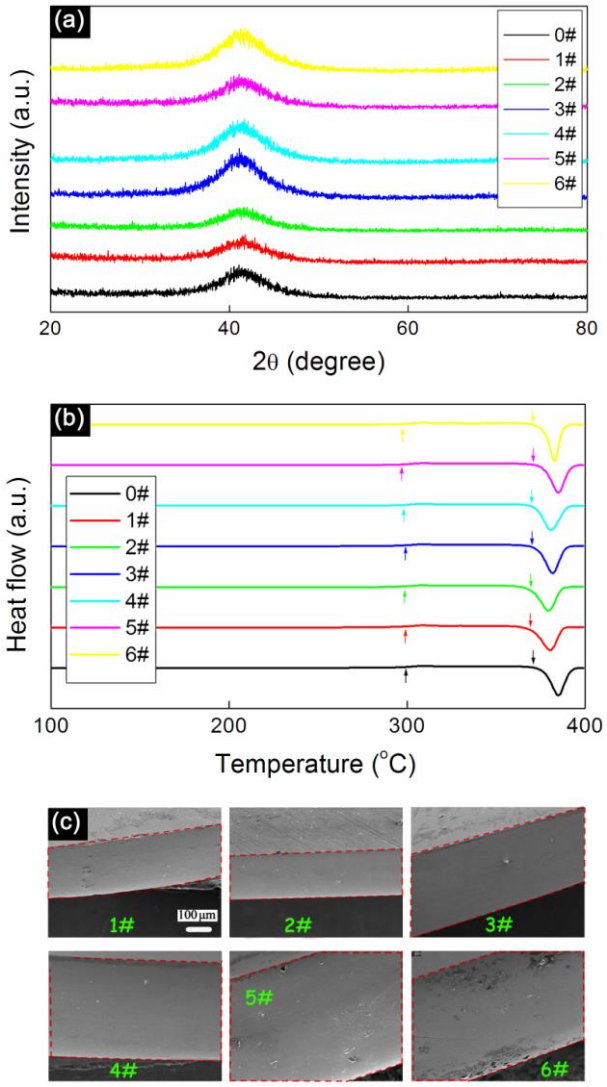

Figure 2. J. Ma *et al*

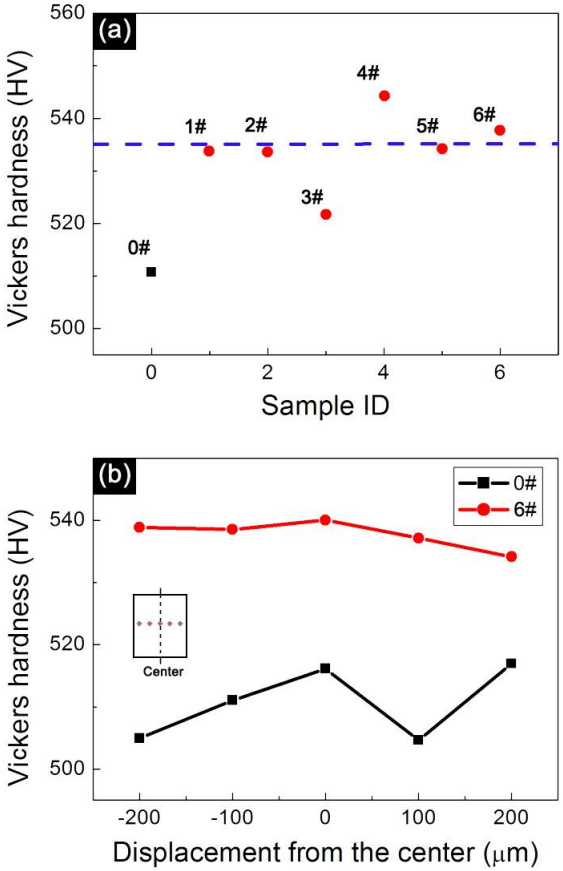

Figure 3. J. Ma *et al*

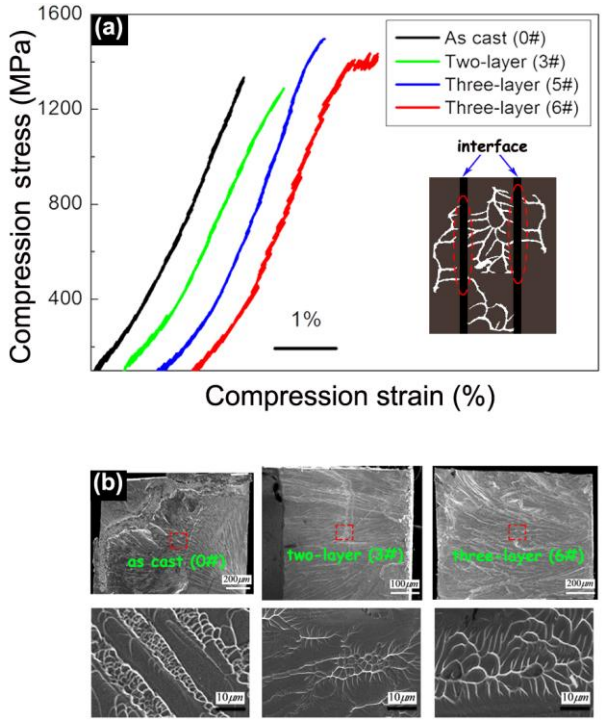

Figure 4. J. Ma *et al*

Table I: Bonding conditions of different samples.

Sample No.	Temperature [K]	Initial pressure [MPa]	Holding time	Layers
0#		As cast		
1#	593	100	10 min	Two
2#	593	50	10 min	Two
3#	593	100	1 min	Two
4#	583	50	10 min	Two
5#	583	50	1 min	Three
6#	583	50	10 s	Three